Current Biology, Volume *31*

Supplemental Information

Chromosome choreography during the non-binary cell cycle of a predatory bacterium

Jovana Kaljević, Terrens N.V. Saaki, Sander K. Govers, Ophélie Remy, Renske van Raaphorst, Thomas Lamot, and Géraldine Laloux

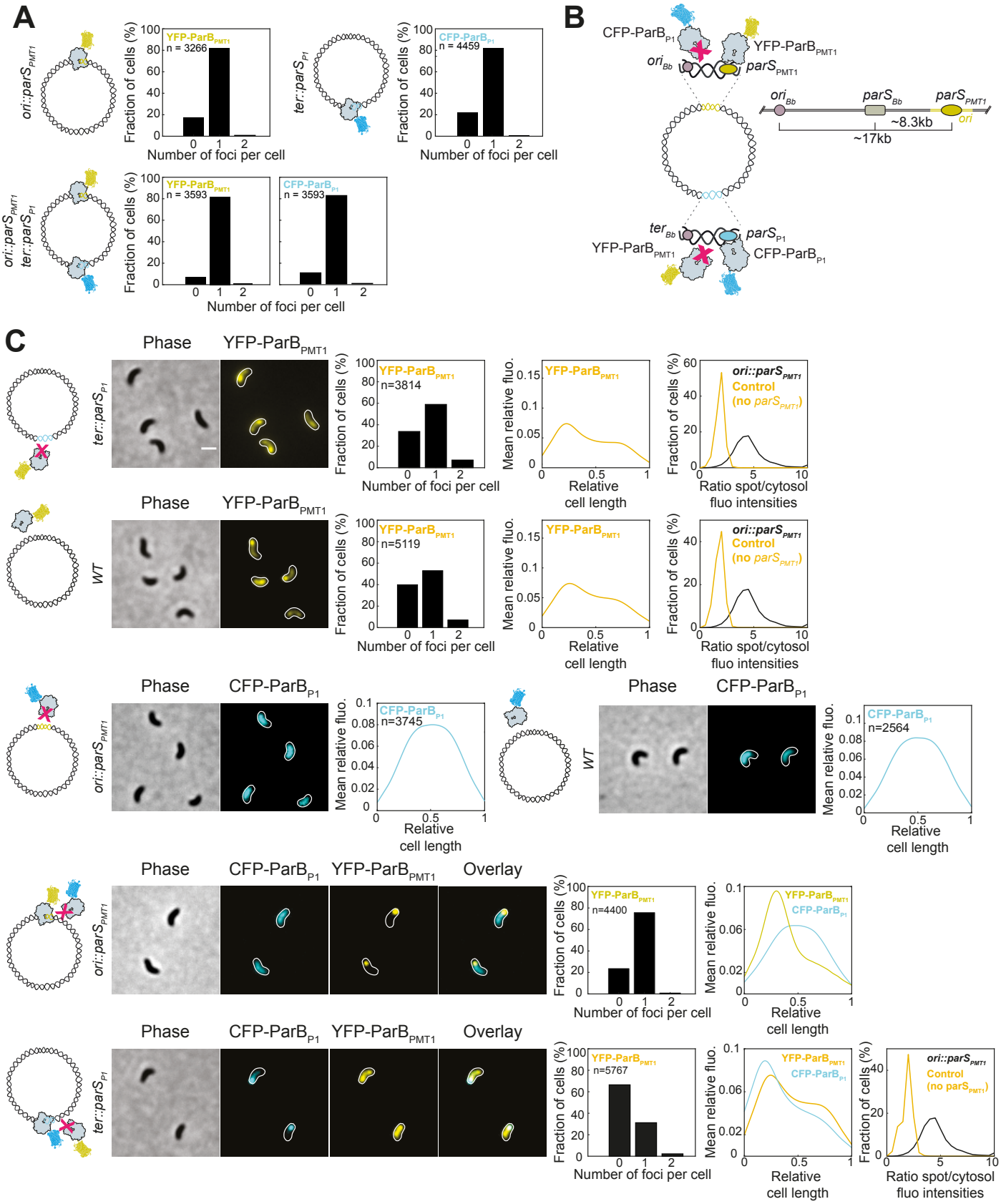
A
ori::parS_PMT1
YFP-ParB_PMT1
n = 3266
Fraction of cells (%)
Number of foci per cell
ter::parS_P1
CFP-ParB_P1
n = 4459
ori::parS_PMT1
ter::parS_P1
n = 3593
B
CFP-ParB_P1
YFP-ParB_PMT1
ori_Bb
parS_PMT1
parS_Bb
~8.3kb
~17kb
ori
ter_Bb
parS_P1
C
Phase
YFP-ParB_PMT1
n=3814
n=5119
Mean relative fluo.
Relative cell length
ori::parS_PMT1
Control
(no parS_PMT1)
Ratio spot/cytosol fluo intensities
WT
CFP-ParB_P1
n=3745
n=2564
n=4400
n=5767
Overlay

Figure S1. **Specificity of the orthologous *parS*-ParB labelling system. Related to Figure 1.** (A) Histograms representing the percentage of cells with zero, one or two YFP-ParB$_{PMT1}$, or CFP-ParB$_{P1}$ foci per cell in strains *ori::parS$_{PMT1}$ /*pTNV215-*yfp-parB$_{PMT1,}$ ter::parS$_{P1}$/*pTNV215-*cfp-parB$_{P1}$* and *ori::parS$_{PMT1}$ ter::parS$_{P1}$ /*pTNV215-*yfp-parB$_{PMT1}$-cfp-parB$_{P1}$* (GL868, GL771 and GL995, respectively). All foci were observed at the poles. The small fractions of cells without focus failed to match stringent spot detection parameters in Oufti. (B) Schematic overview of the orthologous *parS*-ParB pairs as in Fig 1B and controls. From left to right: only specific interactions between the corresponding pairs form a clear fluorescent focus after imaging; schematics of the relative genomic positions of *ori$_{Bb}$* (pink), endogenous *parS$_{Bb}$* (grey) and integrated orthologous *parS$_{PMT1}$* (yellow). (C) Control experiments for *parS*-ParB specific binding. Left to right (from the top): representative phase contrast and fluorescence images of AP cells of strain *ter::parS$_{P1}$* expressing non-cognate YFP-ParB$_{PMT1}$ (GL772); histograms of cells with zero, one or two YFP-ParB$_{PMT1}$ foci; profile as in Fig 1C; distribution of the ratio of YFP-ParB$_{PMT1}$ fluorescence intensity in the spot *vs* in the cytosol measured in cells with one detected focus (orange line: GL772, black line: GL868). As above for cells expressing YFP-ParB$_{PMT1}$ in a wild-type (*WT*) background (strain GL785); orange line: GL785, black line: GL868. Images and profile as above for strain *ori::parS$_{PMT1}$* expressing non-cognate CFP-ParB$_{P1}$ (GL867), which localizes on the nucleoid. As above for cells expressing CFP-ParB$_{P1}$ in a wild-type (*WT)* background (GL784). Images, histogram, and profiles for the indicated fusions for *ori::parS$_{PMT1}$* cells expressing non-cognate CFP-ParB$_{P1}$ and cognate YFP-ParB$_{PMT1}$ (GL869). Representative phase contrast and fluorescence images of AP cells of strain *ter::parS$_{P1}$* expressing cognate CFP-ParB$_{P1}$ and non-cognate YFP-ParB$_{PMT1}$ (GL773); orange line in the ratio distribution plot: GL773, black line: GL868. Schematics illustrate the *ori* and *ter* labelling construct used in each panel. Scale bars are 1 µm. n indicate the number of cells analysed in a representative experiment. Experiments were performed at least twice. For histograms: using the same parameters for automated spot detection as in Fig 1C, YFP-ParB$_{PMT1}$ spots were detected in a lower fraction of control cells lacking the cognate *parS$_{PMT1}$*. Analysis showed that these spots are distinct from the foci seen in strain GL868 (which carries *parS$_{PMT1}$*), supporting the idea that polar accumulations in control strains are non-specific: (1) mean oriented profiles of relative YFP-ParB$_{PMT1}$ fluorescence intensity show less difference between the region containing the highest fluorescence and the rest of the cell, compared to the profile in Fig 1C for strain GL868, and (2) distributions of the ratio of YFP-ParB$_{PMT1}$ fluorescence intensity in the spot *vs* in the cytosol show that spots detected in GL868 (black line) have higher intensity than spots in control strains (orange lines). Of note, CFP-ParB$_{P1}$ produced in the absence of its cognate *parS$_{P1}$* sequence appears nucleoid-bound. All cell outlines were obtained with Oufti.

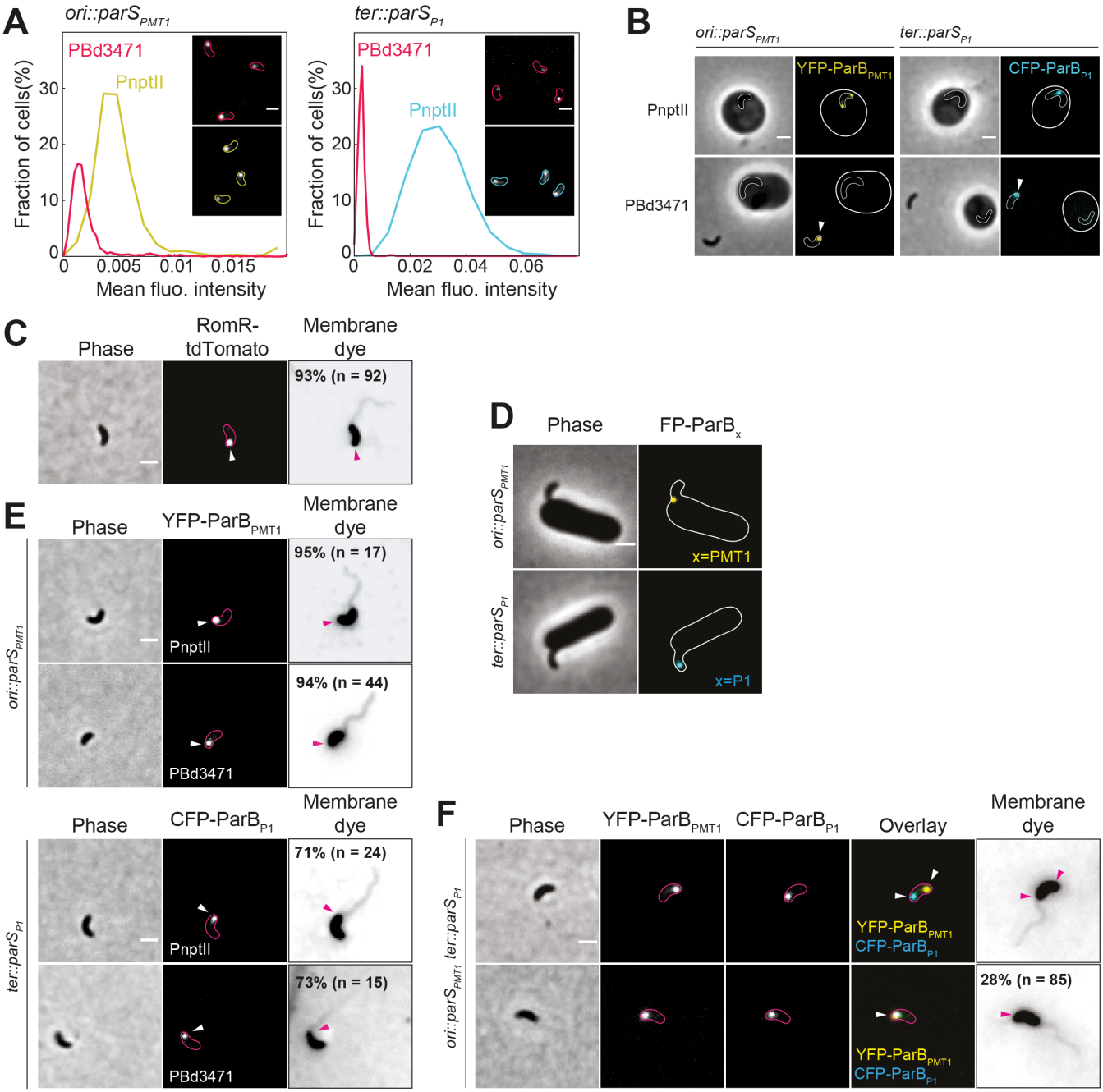
A
ori::parS PMT1
PBd3471
PnptII
Fraction of cells(%)
Mean fluo. intensity
ter::parS P1
PBd3471
PnptII
Fraction of cells(%)
Mean fluo. intensity
B
ori::parS PMT1
ter::parS P1
PnptII
PBd3471
YFP-ParB PMT1
CFP-ParB P1
C
Phase
RomR-tdTomato
Membrane dye
93% (n = 92)
D
Phase
FP-ParB x
ori::parS PMT1
ter::parS P1
x=PMT1
x=P1
E
Phase
YFP-ParB PMT1
Membrane dye
ori::parS PMT1
PnptII
95% (n = 17)
PBd3471
94% (n = 44)
Phase
CFP-ParB P1
Membrane dye
ter::parS P1
PnptII
71% (n = 24)
PBd3471
73% (n = 15)
F
Phase
YFP-ParB PMT1
CFP-ParB P1
Overlay
Membrane dye
ter::parS P1
ori::parS PMT1
YFP-ParB PMT1
CFP-ParB P1
28% (n = 85)

Figure S2. Localization of *ori* and *ter* markers with lower ParB-FP levels, and localization of *ori* and *ter* markers during prey attachment and upon flagellum staining. Related to Figure 1. (A-B) $ParB_{PMT1}$ and $ParB_{P1}$ fusions expressed from a *Bdellovibrio* promoter are produced at low levels and label *ori*::$parS_{PMT1}$ and *ter*::$parS_{P1}$ only in attack phase. (A) Distributions of mean fluorescence intensity values for cells with one detected fluorescent spot: left: AP cells of *ori::*$parS_{PMT1}$ strains expressing cognate YFP-$ParB_{PMT1}$ from PBd3471 (GL1476, red) or the constitutively active promoter PnptII (GL868, yellow); right: AP cells of *ter::*$parS_{P1}$ strains expressing cognate CFP-$ParB_{P1}$ from the PBd3471 promoter (GL1475, red) or PnptII promoter (GL771, cyan); representative images are shown. (B) Representative phase contrast and fluorescence images for the same cells as in A during growth phase (GP). Cells were imaged 3 h after mixing with prey. Arrowheads point to foci in AP *B. bacteriovorus* cells (in contrast with the absence of signal in the GP cell on the same image). (C) RomR is a marker of the invasive pole. Representative phase contrast and fluorescence images of AP cells of cells constitutively producing cognate RomR-TdTomato from a plasmid in *WT* background (strain GL512) prior labelling with CellBrite™ Fix 488 membrane dye. Arrowhead points to the RomR-tdTomato polar focus. (D) As in Figure 1F for *ori::*$parS_{PMT1}$ and *ter::*$parS_{P1}$ strains producing cognate YFP-$ParB_{PMT1}$ or CFP-$ParB_{P1}$ (strains GL868 and GL771, respectively). (E) Representative phase contrast and fluorescence images of strains GL868, GL1476, GL771 and GL1475 after staining with FM4-64 (see genotypes in legend of panel A); the tagged loci and promoters controlling the expression of corresponding ParB fusions are indicated; arrowheads point to polar foci. (F) Same as in Figure 1G for the *ori::*$parS_{PMT1}$ *ter::*$parS_{P1}$ strain constitutively producing cognate CFP-$ParB_{P1}$ and YFP-$ParB_{PMT1}$ from the PnptII promoter (strain GL995); the top and bottom parts represent the most and least frequent configurations, respectively (fraction of cells with colocalized *ori* and *ter* is indicated). Scale bars are 1 µm. n indicate the number of cells analysed manually in a representative experiment. All outlines of bdelloplasts were drawn manually based on phase contrast images; All cell outlines of AP *Bdellovibrio* cells were obtained with Oufti.

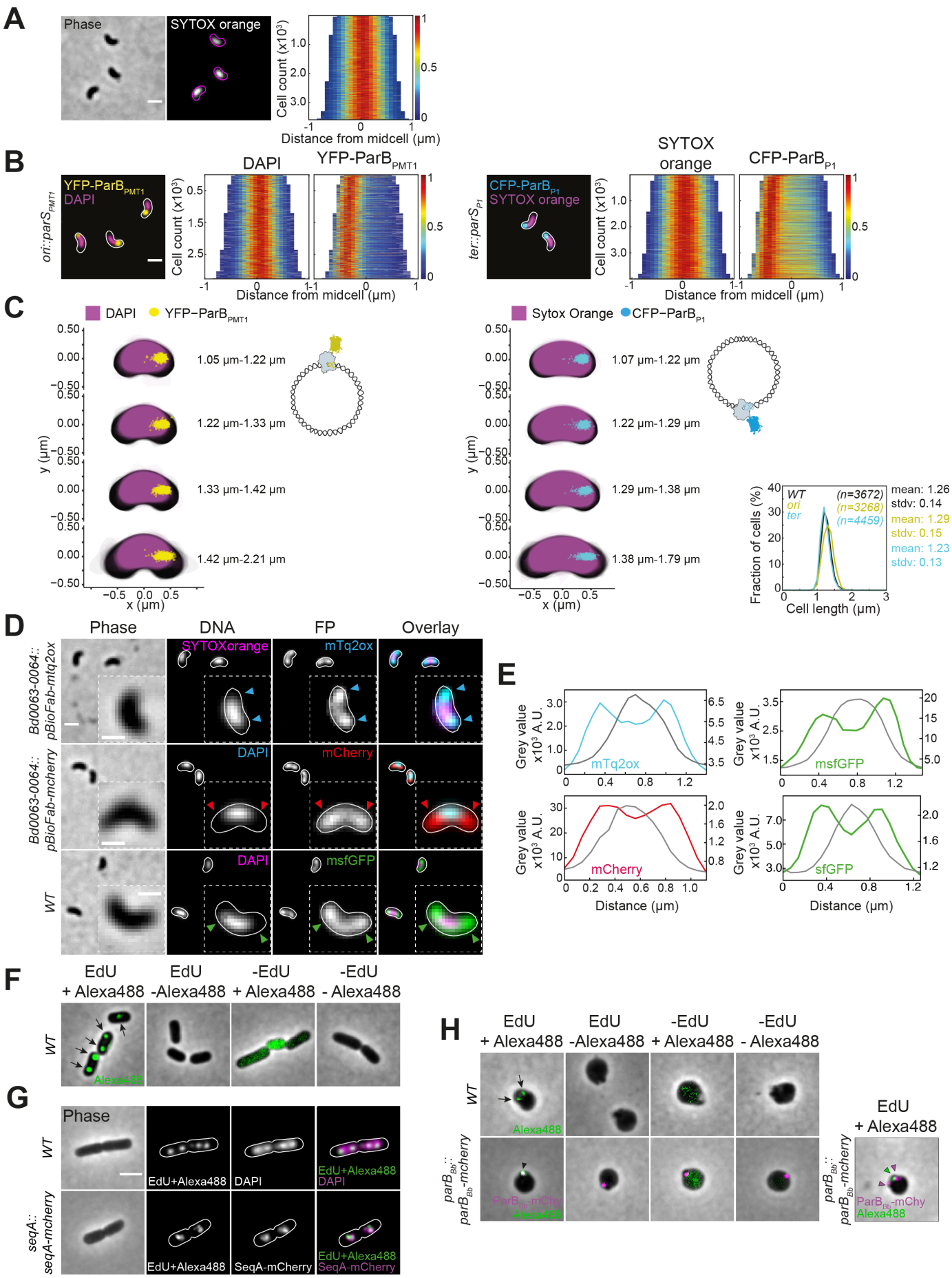
A
Phase
SYTOX orange
Cell count (x10³)
Distance from midcell (µm)
B
DAPI
YFP-ParB$_{PMT1}$
ori::parS$_{PMT1}$
SYTOX orange
CFP-ParB$_{P1}$
ter::parS$_{P1}$
Distance from midcell (µm)
C
DAPI
YFP−ParB$_{PMT1}$
1.05 µm-1.22 µm
1.22 µm-1.33 µm
1.33 µm-1.42 µm
1.42 µm-2.21 µm
Sytox Orange
CFP−ParB$_{P1}$
1.07 µm-1.22 µm
1.22 µm-1.29 µm
1.29 µm-1.38 µm
1.38 µm-1.79 µm
x (µm)
y (µm)
Fraction of cells (%)
Cell length (µm)
WT (n=3672) mean: 1.26 stdv: 0.14
ori (n=3268) mean: 1.29 stdv: 0.15
ter (n=4459) mean: 1.23 stdv: 0.13
D
Phase
DNA
FP
Overlay
Bd0063-0064::pBioFab-mtq2ox
Bd0063-0064::pBioFab-mcherry
WT
SYTOXorange
mTq2ox
DAPI
mCherry
msfGFP
E
Grey value x10³ A.U.
mTq2ox
msfGFP
mCherry
sfGFP
Distance (µm)
F
EdU + Alexa488
EdU -Alexa488
-EdU + Alexa488
-EdU - Alexa488
WT
Alexa488
G
Phase
EdU+Alexa488
DAPI
EdU+Alexa488 DAPI
seqA::seqA-mcherry
SeqA-mCherry
EdU+Alexa488 SeqA-mCherry
H
parB$_{Bb}$::parB$_{Bb}$-mcherry
ParB$_{Bb}$-mChy
Alexa488

Figure S3. Nucleoid compaction in *B. bacteriovorus*. Related to Figure 2 and Figure 3. (A) Left to right: representative phase contrast and fluorescence images of AP cells of *WT B. bacteriovorus* stained with SYTOX orange; demograph of the corresponding fluorescent signal in the same cells. Heatmaps represent relative fluorescence intensities. (B) Key chromosomal loci, *ori* and *ter* localize at the nucleoid tips. Images shown in Figure 2C. Demographs of the corresponding fluorescent signals in the same cells, oriented based on signal intensity of the indicated ParB fusion. Heatmaps represent relative fluorescence intensities. (C) Projections where cells were grouped by cell length and cell shape, each projected stack of cells including DNA-staining shape and fluorescent spots as indicated. Bottom right: histograms of cell lengths for WT (HD100), *ori::parS*$_{PMT1}$/pTNV215-*yfp-parB*$_{PMT1}$ (GL868) and *ter::parS*$_{P1}$/pTNV215-*cfp-parB*$_{P1}$ (GL771) strains; mean and standard deviation values are shown; n indicate the number of cells analysed for each strain in a representative experiment. Schematics illustrate the *ori* and *ter* labelling constructs used in this panel. (D) Partial nucleoid exclusion of free fluorescent proteins. Representative phase contrast and fluorescence images of strains *Bd0063-0064::pBioFab-sftq2ox* and *Bd0063-0064::pBioFab-mcherry* (GL1024 and GL1025, respectively), or *WT/*pTNV215-*msfgfp* (GL1208) stained with SYTOX orange or DAPI as indicated. Arrowheads point to nucleoid exclusions on an enlarged example (inset). Scale bar is 1 µm except for enlarged examples where scale bar is 0.5 µm. (E) Fluorescence intensity profiles of the corresponding signals in representative cells from D and Figure 2E. (F-H) The nucleoside analogue EdU marks areas within the cell where new DNA is being synthesized, positive and negative controls in *E. coli.* (F) Representative overlays of phase contrast and fluorescence images of *WT* strain exposed to a 15-minute pulse of EdU and Alexa488 in different combinations; arrows point to foci of Alexa488-labeled EdU; no Alexa488 foci were observed in the absence of EdU. (G) *WT* and *seqA::seqA-mCherry* strains, exposed to a 15-minute pulse of EdU, which was fluorescently labelled with Alexa488 and stained with DAPI when indicated. EdU-Alexa488 and SeqA-mCherry foci colocalize. (H) The nucleoside analogue EdU marks areas within the cell where new DNA is being synthesized in *B. bacteriovorus.* Representative overlays of phase contrast and fluorescence images of *WT* and *parB*$_{Bb}$*::parB*$_{Bb}$*-mCherry* (GL906) strains 150 min after mixing with prey, in both cases, and exposed to a 5-minute pulse of the EdU and Alexa488 in different combinations; arrows point two foci of Alexa488-labeled EdU; arrowheads point to the colocalization of one focus of EdU, which was fluorescently labelled with Alexa488, and one or two ParB$_{Bb}$-mCherry, respectively which mark the position of *oriC.* Scale bar is 2 µm, applicable to all panels. For all, cell outlines of AP *Bdellovibrio* cells were obtained with Oufti.

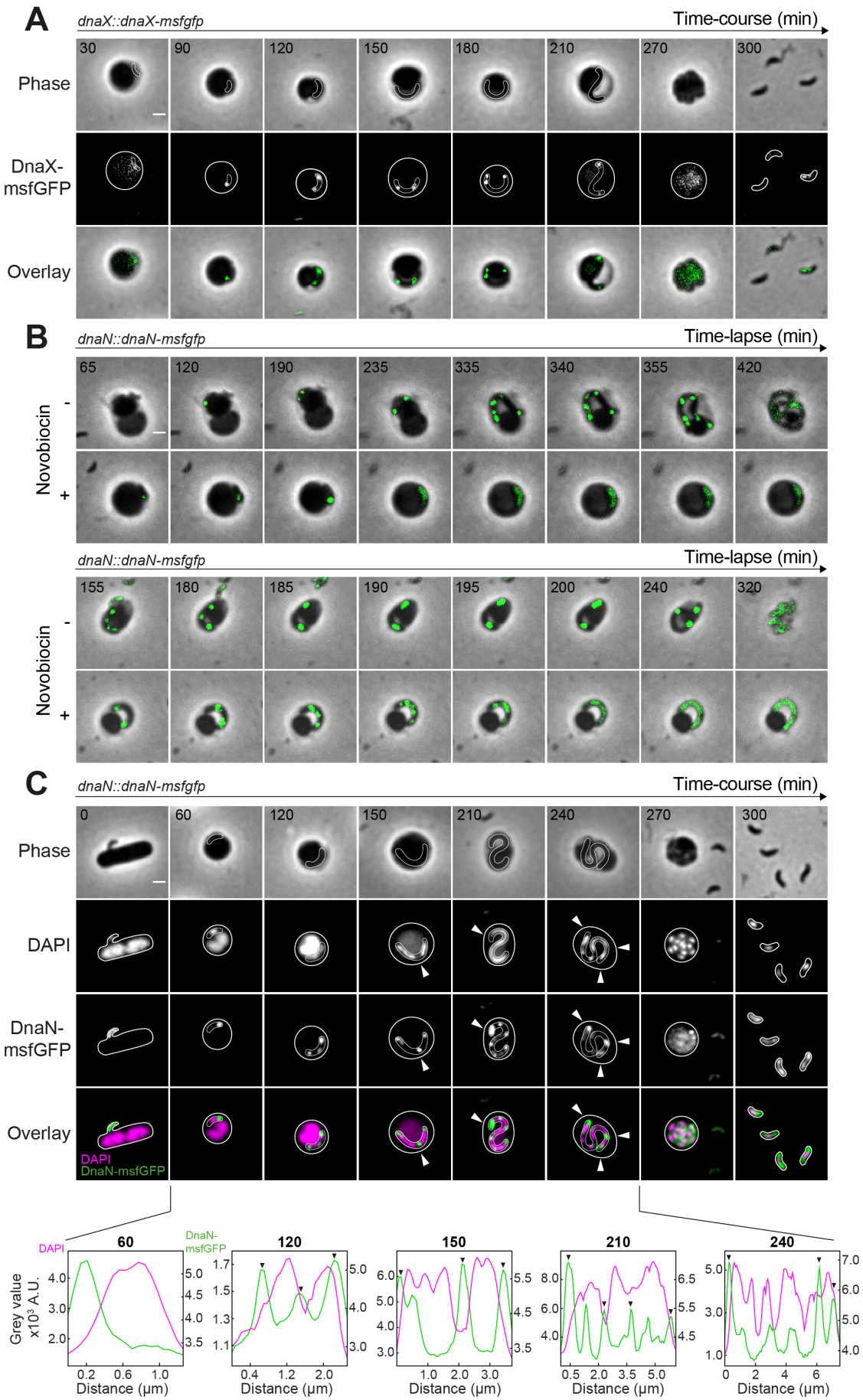
A
dnaX::dnaX-msfgfp
Time-course (min)
Phase
DnaX-msfGFP
Overlay
30
90
120
150
180
210
270
300
B
dnaN::dnaN-msfgfp
Time-lapse (min)
Novobiocin
-
+
65
120
190
235
335
340
355
420
155
180
185
190
195
200
240
320
C
dnaN::dnaN-msfgfp
Time-course (min)
Phase
DAPI
DnaN-msfGFP
Overlay
0
60
120
150
210
240
270
300
DAPI
DnaN-msfGFP
Grey value x10³ A.U.
Distance (µm)

Figure S4. Replisome dynamics and nucleoid localization in *B. bacteriovorus.* Related to Figure 4. (A) Localization dynamics of DnaX in *B. bacteriovorus. B. bacteriovorus* strain *dnaX::dnaX-msfgfp* (GL1364) was mixed with prey and imaged in time-course every 30 min after mixing with prey; phase contrast and fluorescence images of selected timepoints from a representative experiment are shown. Scale bar is 1 µm. (B) Gyrase inhibitor novobiocin prevents new rounds of DNA replication initiation. *B. bacteriovorus* strain *dnaN::dnaN-msfgfp* (GL673) was mixed with prey, not treated (-) or treated (+) with 5 µg/ml novobiocin (top) 65 min after mixing with prey or (bottom) 155 min after mixing with prey, before time-lapse imaging at 5 min intervals on agarose pads containing 5 µg/ml novobiocin (+) or not (-). Phase contrast and fluorescence images of selected timepoints of a representative experiment are shown. Inhibitory effect is indicated by a disassembly of the existing DnaN-msfGFP foci and the absence of new foci formation. Scale bar is 1 µm. (C) DAPI staining in cells with labelled replisome. *B. bacteriovorus* strain *dnaN::dnaN-msfgfp* (GL673) was mixed with prey and imaged in time-course at 30 min intervals. Top: phase contrast and fluorescence images of selected timepoints from a representative experiment are shown; arrowheads point to regions with less DAPI signal and where replisomes are located. Scale bar is 1 µm. For all, outlines of *B. bacteriovorus* and bdelloplasts were drawn manually based on phase contrast images. Bottom: fluorescence intensity profiles of the corresponding signals in the same cells; arrowheads point to regions with less DAPI signal and where replisomes are located.

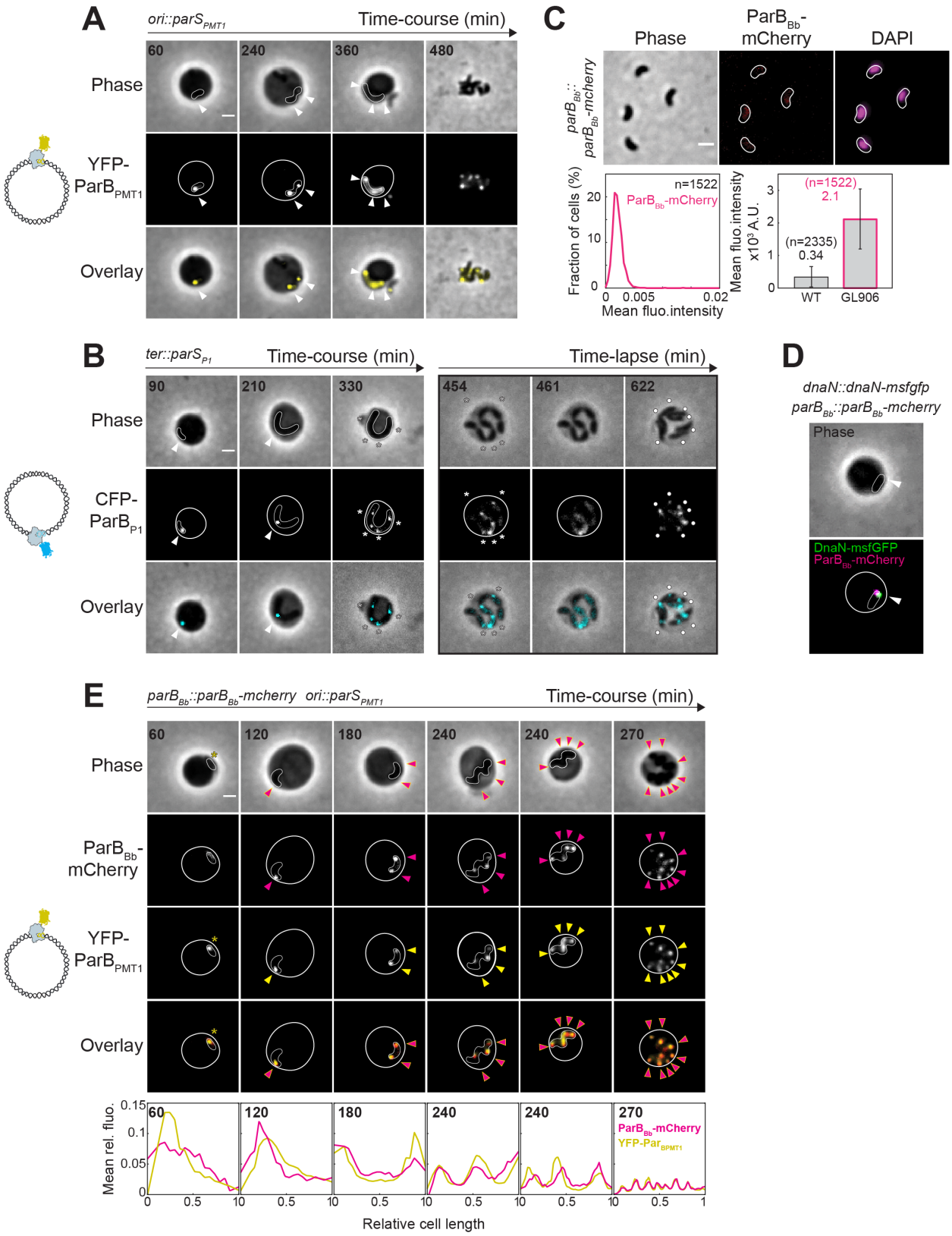
A
ori::parS PMT1
Time-course (min)
60
240
360
480
Phase
YFP-ParB PMT1
Overlay
B
ter::parS P1
Time-course (min)
Time-lapse (min)
90
210
330
454
461
622
Phase
CFP-ParB P1
Overlay
C
Phase
ParB Bb-mCherry
DAPI
parB Bb::parB Bb-mcherry
Fraction of cells (%)
n=1522
ParB Bb-mCherry
Mean fluo.intensity
Mean fluo.intensity x10³ A.U.
(n=1522) 2.1
(n=2335) 0.34
WT
GL906
D
dnaN::dnaN-msfgfp
parB Bb::parB Bb-mcherry
Phase
DnaN-msfGFP
ParB Bb-mCherry
E
parB Bb::parB Bb-mcherry ori::parS PMT1
Time-course (min)
60
120
180
240
240
270
Phase
ParB Bb-mCherry
YFP-ParB PMT1
Overlay
Mean rel. fluo.
ParB Bb-mCherry
YFP-Par BPMT1
Relative cell length

Figure S5. Spatio-temporal arrangement of the chromosome during the S phase and $ParB_{Bb}$ localization in AP cells. Related to Figure 5. (A) After a first asymmetric segregation, additional *ori* foci appear. *B. bacteriovorus* strain *ori::parS*$_{PMT1}$ expressing cognate YFP-$ParB_{PMT1}$ (GL868) was mixed with prey and imaged in time-course with 30 min intervals. Phase contrast and fluorescence images of selected timepoints of a representative experiment are shown; arrowheads point to fluorescent foci. (B) *ter* dynamics during the proliferative phase. *B. bacteriovorus* strain *ter::parS*$_{P1}$ expressing cognate CFP-$ParB_{P1}$ (GL771) was mixed with prey and imaged in time-course with 30 min intervals (left) or time-lapse after 90 min with 7 min intervals (right). For each, phase contrast and fluorescence images of selected timepoints of a representative experiment are shown; arrowheads point to polar then mid-cell *ter* localization; asterisks point to evenly distributed *ter* copies; timepoint 461 min from time-lapse illustrates *ter* foci disassembly; circles point to re-appearance of *ter* foci in daughter cells. (C) Endogenous $ParB_{Bb}$ does not form an *ori*-bound focus during AP. Representative phase contrast and fluorescence images of attack phase cells of *parB*$_{Bb}$::*parB*$_{Bb}$*-mcherry* strain (GL906) stained with DAPI; histogram of mean fluorescence intensity of the corresponding signal in the same cells; mean mCherry fluorescence intensity in the same GL906 cells compared to *WT;* n indicate the number of cells analysed in a representative experiment; mean values are represented. Error bars indicate standard deviations. Cell outlines were obtained with Oufti. (D) Endogenous $ParB_{Bb}$ forms a focus that colocalizes with the replisome at the start of the S phase. Representative phase contrast and fluorescence images of *dnaN::dnaN-msfgfp parB*$_{Bb}$*::parB*$_{Bb}$*-mcherry* strain (GL1055) imaged 110 min after mixing with *E. coli* prey; colocalization in 93% (n=111 from one representative experiment, colocalization was quantified manually). (E) $ParB_{Bb}$-mCherry is *bona fide* marker of *ori* in *Bdellovibrio bacteriovorus. B. bacteriovorus* strain *parB*$_{Bb}$*::parB*$_{Bb}$*-mcherry ori::parS*$_{PMT1}$ expressing cognate YFP-$ParB_{PMT1}$ (GL1367) was mixed with prey and imaged in time-course with 30 min intervals. Top: phase contrast and fluorescence images of selected timepoints from a representative experiment are shown; both signals colocalized through the cycle (pink and yellow arrowheads), except in the early stages where only signal from YFP-$ParB_{PMT1}$ was visible (yellow asterisk). Bottom: mean pole-to-pole profiles of relative fluorescence intensity of the corresponding fusions in the same cells. Schematics illustrate the *ori* and *ter* labelling constructs used in appropriate panels. Scale bars are 1 µm. For all, except in C, outlines of *B. bacteriovorus* and bdelloplasts were drawn manually based on phase contrast images.

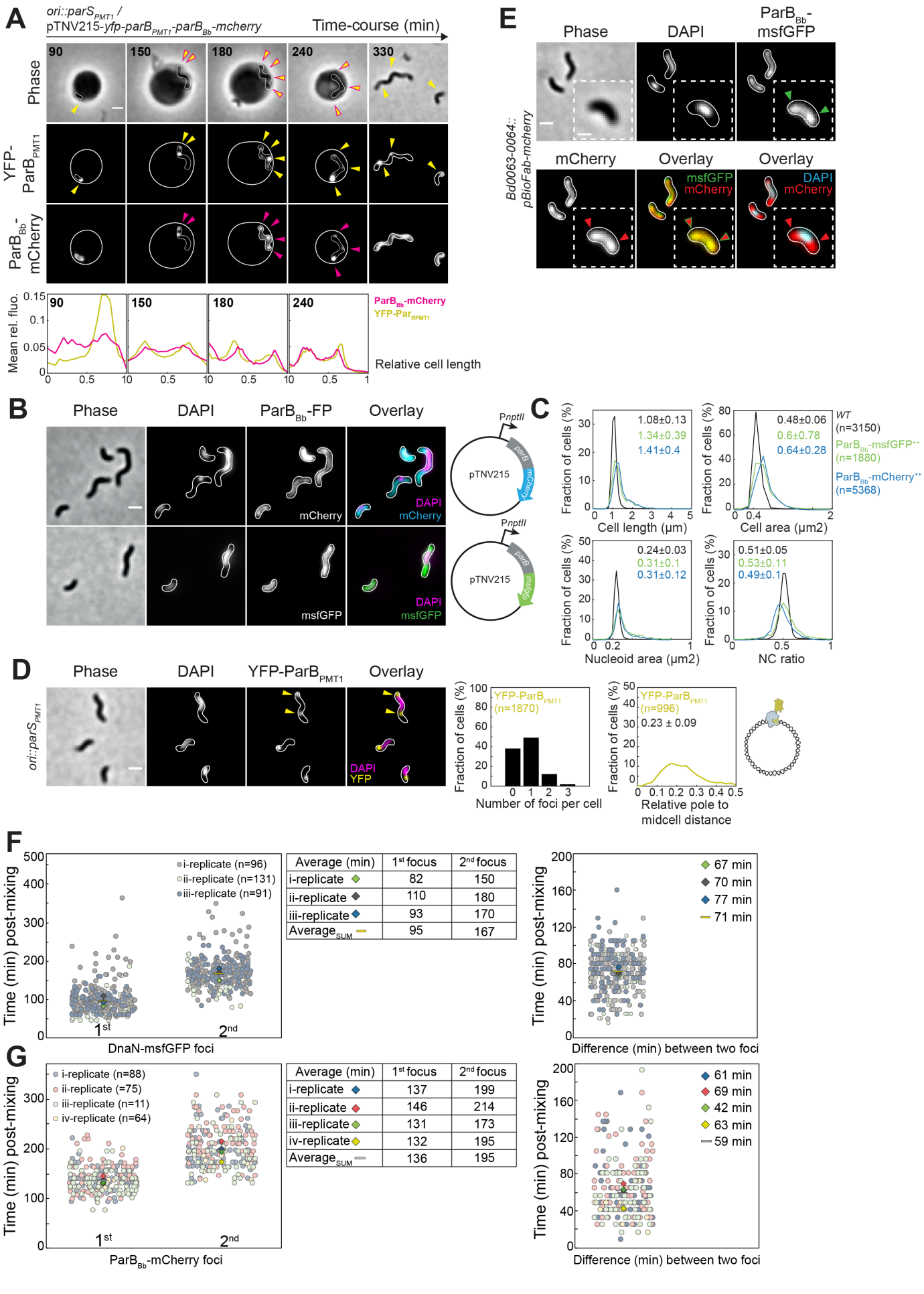
A
ori::parS_PMT1 /
pTNV215-yfp-parB_PMT1-parB_Bb-mcherry
Time-course (min)
90
150
180
240
330
Phase
YFP-ParB_PMT1
ParB_Bb-mCherry
Mean rel. fluo.
ParB_Bb-mCherry
YFP-Par_BPMT1
Relative cell length
B
Phase
DAPI
ParB_Bb-FP
Overlay
mCherry
msfGFP
DAPI
PnptII
pTNV215
parB
mCherry
msfGFP
C
Fraction of cells (%)
1.08±0.13
1.34±0.39
1.41±0.4
Cell length (µm)
0.48±0.06
0.6±0.78
0.64±0.28
Cell area (µm2)
WT
(n=3150)
ParB_Bb-msfGFP++
(n=1880)
ParB_Bb-mCherry++
(n=5368)
0.24±0.03
0.31±0.1
0.31±0.12
Nucleoid area (µm2)
0.51±0.05
0.53±0.11
0.49±0.1
NC ratio
D
ori::parS_PMT1
Phase
DAPI
YFP-ParB_PMT1
Overlay
YFP
YFP-ParB_PMT1
(n=1870)
Number of foci per cell
(n=996)
0.23 ± 0.09
Relative pole to
midcell distance
E
Bd0063-0064::
pBioFab-mcherry
Phase
DAPI
ParB_Bb-
msfGFP
mCherry
Overlay
msfGFP
mCherry
DAPI
mCherry
F
Time (min) post-mixing
i-replicate (n=96)
ii-replicate (n=131)
iii-replicate (n=91)
1st
2nd
DnaN-msfGFP foci
Average (min) | 1st focus | 2nd focus
i-replicate | 82 | 150
ii-replicate | 110 | 180
iii-replicate | 93 | 170
Average_SUM | 95 | 167
67 min
70 min
77 min
71 min
Difference (min) between two foci
G
i-replicate (n=88)
ii-replicate (=75)
iii-replicate (n=11)
iv-replicate (n=64)
ParB_Bb-mCherry foci
Average (min) | 1st focus | 2nd focus
i-replicate | 137 | 199
ii-replicate | 146 | 214
iii-replicate | 131 | 173
iv-replicate | 132 | 195
Average_SUM | 136 | 195
61 min
69 min
42 min
63 min
59 min

Figure S6. The ParABS system contributes to progressive *ori* segregation. Related to Figure 6. (A) Foci formed by overproduced $ParB_{Bb}$-mCherry label *ori*. Top: time-course experiment of an *ori::parS$_{PMT1}$* strain constitutively expressing YFP-$ParB_{PMT1}$ and $ParB_{Bb}$-mCherry (GL1372); both signals colocalized through the cycle (pink and yellow arrowheads), except in the early stages where foci were visible only for YFP- $ParB_{PMT1}$ (yellow arrowhead); cells were mixed with prey and imaged at 30 min intervals; selected frames are presented. Bottom: mean pole-to-pole profiles of relative fluorescence intensity of the corresponding fusions in the same cells. n indicate the number of cells analysed in a representative experiment. (B) Overproduction of $ParB_{Bb}$ leads to phenotypic changes in AP cells. Representative phase contrast and fluorescence images of AP cells of *WT* strains constitutively expressing $ParB_{Bb}$-mCherry (top) and $ParB_{Bb}$-msfGFP (bottom) stained with DAPI (GL1002 and GL1003, respectively). (C) Overexpression of $ParB_{Bb}$ leads to pronounced phenotypes. Histograms of cell length, cell area, nucleoid area and NC ratio for the cells shown in B; mean and standard deviation values are shown. (D) Overexpression of $ParB_{Bb}$ leads to aberrant numbers of *ori* copies in AP cells. From left to right: representative phase contrast and fluorescence images of AP cells of the same strain shown in A (GL1372) stained with DAPI; arrowheads point to *ori* foci; histograms representing the proportion of cells with zero, one or two YFP-$ParB_{PMT1}$ foci in the same cells; relative pole to mid-cell distance profile for YFP- $ParB_{PMT1}$ in the same cells. Fluorescent signal from $ParB_{Bb}$-mCherry is not shown for simplicity, both signals always colocalized (see A). Schematics illustrate the *ori* labelling construct. (E) Partial nucleoid exclusion of cytoplasmic fluorescent proteins in $ParB_{Bb}$ overproducing strain. Representative phase contrast and fluorescence images of strain *Bd0063-0064::pBioFab-mcherry/*pTNV215-*parB$_{Bb}$-msfgfp* (GL1388) stained with DAPI. Arrowheads point to nucleoid exclusions on an enlarged example (inset). (F) Dynamics of chromosome replication. SuperPlot representation of the time of appearance of first and second DnaN-msfGFP focus in strain *dnaN::dnaN-msfgfp* (GL673) (left), and the time difference between appearance of first and second DnaN-msfGFP foci in the same cells (right). (G) Dynamics of chromosome segregation. SuperPlot representation of the time of appearance of first and second $ParB_{Bb}$-mCherry focus in strain *parB$_{Bb}$::parB$_{Bb}$-mcherry* (GL906) (left), and the time difference between appearance of first and second $ParB_{Bb}$-mCherry foci in the same cells (right). (F-G) Each biological replicate is color-coded; the average from each replicate is represented as a colored diamond and the mean values obtained from all replicates averages are represented as bars. Calculated values are summarized in the corresponding tables; n indicate the number of cells analyzed in each experiment. Scale bars are 1 µm except for enlarged examples where scale bar is 0.5 µm. Outlines of *B. bacteriovorus* and bdelloplasts were obtained with Oufti, except in A where they were drawn manually based on phase contrast images. Experiments were performed at least twice.

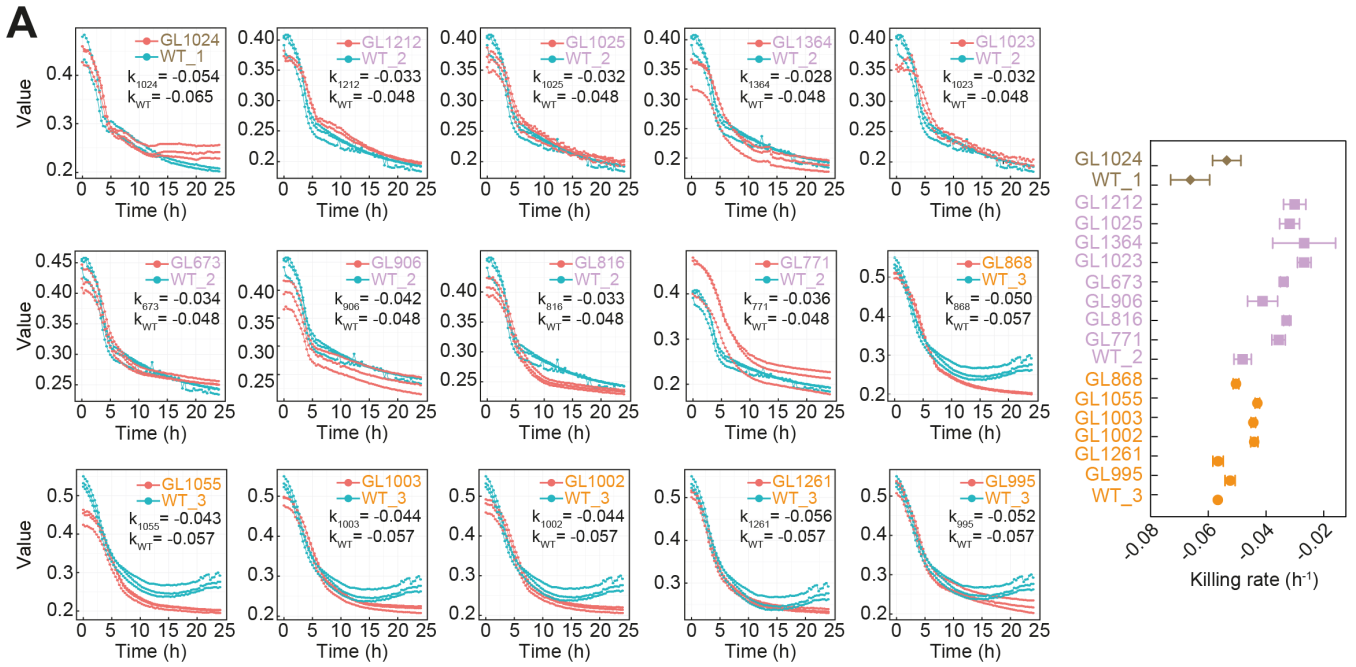

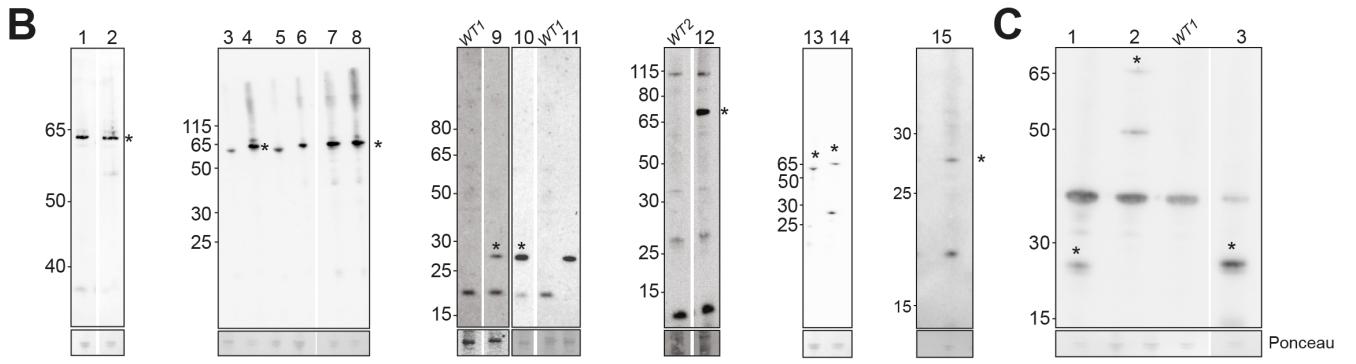

α-GFP
- CFP-ParB$_{P1}$ (61,8 kDa): lanes 1, 2, 4, 6, 7, 8
- YFP-ParB$_{PMT1}$ (61 kDa): lanes 3, 4, 5, 7, 8, 13
- DnaN-msfGFP (68,7 kDa): lane 12
- ParB$_{Bb}$-msfGFP (63,9 kDa): lane 14
- sfTurquoise2ox (26,8 kDa): lane 9
- msfGFP (26,6 kDa): lane 10, 11
- sfGFP (26,8 kDa): lane 15

α-mCherry
- mCherry (26,6 kDa): lanes 1, 3
- ParB$_{Bb}$-mCherry (63,8 kDa): lane 2

Figure S7. Killing rates of *B. bacteriovorus* strains and Western Blot detection of protein fusions used in this study. **Related to STAR Methods.** (A) Left: killing curves of *WT* cells (cyan) and various *B. bacteriovorus* strains (red). *k* indicates the mean killing rate (h^{-1}) calculated for each strain based on biological replicates (i.e. predator lysates coming from distinct plaques) shown on the graphs, from one representative experiment out of at least two independent repeats. Representative experiments are colour-coded. Right: mean and standard deviations of killing rates (h^{-1}) corresponding to data shown on the left. (B-C) Western blots of whole-cell protein extracts from *B. bacteriovorus* and *E. coli* were probed with α-GFP (B) and α-mCherry (C) antibodies to confirm proper protein production. (B) Lanes 1-15 are for (1) *ter::parS*$_{P1}$/pTNV215-*cfp-parB*$_{P1}$ (GL771), (2) *WT*/pTNV215-*cfp-parB*$_{P1}$ (GL784), (3) *ter::parS*$_{P1}$/pTNV215-*yfp-parB*$_{PMT1}$ (GL772), (4) *ter::parS*$_{P1}$/pTNV215-*yfp-parB*$_{PMT1}$-*cfp-parB*$_{P1}$ (GL773), (5) *WT*/pTNV215-*yfp-parB*$_{PMT1}$ (GL785), (6) *ori::parS*$_{PMT1}$/pTNV215-*cfp-parB*$_{P1}$ (GL867), (7) *ori::parS*$_{PMT1}$/pTNV215-*yfp-parB*$_{PMT1}$-*cfp-parB*$_{P1}$ (GL869), (8) *ori::parS*$_{PMT1}$ *ter::parS*$_{P1}$/pTNV215-*yfp-parB*$_{PMT1}$-*cfp-parB*$_{P1}$ (GL995), (9) *Bd0063-0064::pBioFab-sftq2ox* (GL1024), (10) *WT*/pTNV215-*msfgfp* (GL1208), (11) MG1655/pBAD18-msfgfp (GL726), (12) *dnaN::dnaN-msfgfp* (GL673), (13) *ori::parS*$_{PMT1}$/pTNV215-*yfp-parB*$_{PMT1}$ (GL868), (14) *WT/*pTNV215-*parB*$_{Bb}$-*msfgfp* (GL1003), (15) *Bd0063-0064::pBioFab-sfgfp* (GL1212). (C) Lanes 1-3 are for: (1) *Bd0063-0064::pBioFab-mcherry* (GL1025), (2) *WT/*pTNV215-*parB*$_{Bb}$-*mcherry* (GL1002), (3) *MG1655/*pBAD18-*mcherry* (GL727). *B. bacteriovorus* wild-type controls are shown: GL734 (*WT1*) and GL499 (*WT2)*. Detected proteins and their expected sizes are indicated for each panel. Asterisks are on top or next to full-length protein fusions when non-specific bands are present. Ponceau staining of the same membranes (where bands were most visible, ~30-50 kDa) is illustrated bellow each blot as a loading indicator. Molecular weight markers (kDa) are shown on the side.

Bdellovibrio bacteriovorus			
Strains	**Description**	**Resistance**	**Source or reference**
GL499	HD100	/	ATCC strain 15356
GL512	HD100 / pMQ414-*romR*	Gm	This study
GL734	HD100	/	[S1] (kind gift from R.E. Sockett, U. Nottingham)
GL673	HD100 *dnaN::dnaN-msfgfp*	/	This study
GL676	HD100 *ter*::$parS_{P1}$	/	This study
GL771	HD100 *ter*::$parS_{P1}$ / pTNV215-*cfp-*$parB_{P1}$	Gm	This study
GL772	HD100 *ter*::$parS_{P1}$ / pTNV215-*yfp-*$parB_{PMT1}$	Gm	This study
GL773	HD100 *ter*::$parS_{P1}$ / pTNV215-*yfp-*$parB_{PMT1}$-*cfp-*$parB_{P1}$	Gm	This study
GL784	HD100 / pTNV215-*cfp-*$parB_{P1}$	Gm	This study
GL785	HD100 / pTNV215-*yfp-*$parB_{PMT1}$	Gm	This study
GL806	HD100 *ori*::$parS_{PMT1}$	/	This study
GL816	HD100 *ter*::$parS_{P1}$ / pTNV215-*cfp-*$parB_{P1}$-*romR-tdtomato*	Gm	This study
GL867	HD100 *ori*::$parS_{PMT1}$ / pTNV215-*cfp-*$parB_{P1}$	Gm	This study
GL868	HD100 *ori*::$parS_{PMT1}$ / pTNV215-*yfp-*$parB_{PMT1}$	Gm	This study
GL869	HD100 *ori*::$parS_{PMT1}$ / pTNV215-*yfp-*$parB_{PMT1}$-*cfp-*$parB_{P1}$	Gm	This study
GL870	HD100 *ori*::$parS_{PMT1}$ / pTNV215-*cfp-*$parB_{P1}$-*romR-tdtomato*	Gm	This study
GL906	HD100 $parB_{Bb}$::$parB_{Bb}$-*mcherry*	/	This study
GL909	HD100 *ori*::$parS_{PMT1}$ *ter*::$parS_{P1}$	/	This study
GL995	HD100 *ori*::$parS_{PMT1}$ *ter*::$parS_{P1}$ / pTNV215-*yfp-*$parB_{PMT1}$-*cfp-*$parB_{P1}$	Gm	This study
GL1002	HD100 / pTNV215-$parB_{Bb}$-*mcherry*	Gm	This study
GL1003	HD100 / pTNV215-$parB_{Bb}$-*msfgfp*	Gm	This study
GL1024	HD100 *Bd0063-0064*::*pBioFab-sftq2ox*	/	This study*
GL1025	HD100 *Bd0063-0064*::*pBioFab-mcherry*	/	This study
GL1055	HD100 *parB*::$parB_{Bb}$-*mcherry dnaN::dnaN-msfgfp*	/	This study
GL1102	HD100 *ori*::$parS_{PMT1}$ *dnaN::dnaN-msfgfp*	/	This study
GL1103	HD100 *ori*::$parS_{PMT1}$ *dnaN::dnaN-msfgfp* / pTNV215-*mCherry-*$parB_{PMT1}$	Gm	This study
GL1121	HD100 *parB*::$parB_{Bb}$-*mcherry ori*::$parS_{PMT1}$	/	This study
GL1122	HD100 *parB*::$parB_{Bb}$-*mcherry ter*::$parS_{P1}$	/	This study
GL1208	HD100 / pTNV215-*msfgfp*	Gm	This study
GL1211	HD100 *dnaN*::*dnaN-msfgfp* / pTNV215-*romR-tdtomato*	Gm	This study
GL1212	HD100 *Bd0063-0064*::*pBioFab-sfgfp*	/	This study
GL1261	HD100 / pTNV215-$parB_{Bb}$	Gm	This study
GL1364	HD100 *dnaX::dnaX-msfgfp*	/	This study
GL1367	HD100 *parB*::$parB_{Bb}$-*mcherry ori*::par_{SPMT1} / pTNV215-*yfp-*$parB_{PMT1}$	Gm	This study
GL1368	HD100 *parB*::$parB_{Bb}$-*mcherry ter*::$parS_{P1}$ / pTNV215-*cfp-*$parB_{P1}$	Gm	This study
GL1372	HD100 *ori*::$parS_{PMT1}$ / pTNV215-*yfp-*$parB_{PMT1}$-$parB_{Bb}$-*mcherry*	Gm	This study
GL1388	HD100 *Bd0063-0064*::*pBioFab-mcherry* / pTNV215-$parB_{Bb}$-*msfgfp*	Gm	This study
GL1475	HD100 *ter*::$parS_{P1}$ / pTNV215-*PBd3471-cfp-*$parB_{P1}$	Gm	This study**
GL1476	HD100 ori::$parS_{P1}$ / pTNV215-*PBd3471-yfp-*$parB_{PMT1}$	Gm	This study

E. coli			
Strains	**Description**	**Resistance**	**Source or reference**
S17-1 λ*pir*	Donor strain for conjugative transfer (chromosomally integrated RP4 plasmid)	Strep	Lab collection
MG1655	WT *E. coli* strain used as prey for *B. bacteriovorus*	/	Lab collection
GL503	S17-1 λ*pir* / pXDB013 (pMR-*yfp-parB*$_{PMT1}$-*cfp-parB*$_{P1}$)	Kan	S2
GL504	S17-1 λ*pir* / pXDB014 (pMR-*yfp-parB*$_{PMT1}$)	Kan	S2
GL505	S17-1 λ*pir* / pXDB015 (pMR-*cfp-parB*$_{P1}$)	Kan	S2
GL506	DH10B / pXDB025 (pKS-*oriT-parS*$_{P1}$)	Chlor	S2
GL507	DH10B / pXDB024 (pKS-oriT-parS$_{PMT1}$)	Chlor	S2
GL511	S17-1 λ*pir* / pMQ414-r*omR* (encodes RomR-tdTomato)	Gm	This study
GL573	S17-1 λ*pir* / pPROBE-NT	Kan	S3
GL606	NEB5α / pTNV215-*tdtomato* (*PnptII-tdtomato-RSF1010-oriT-p15A* = pMQ414 without yeast maintenance sequences)	Gm	This study
GL611	S17-1 λ*pir*/ pTNV215-*romR-tdtomato*	Gm	This study
GL630	S17-1 λ*pir* / pK18*mobsacB-Bd3895up-parS*$_{PMT1}$-*Bd3896down*	Kan	This study
GL631	S17-1 λ*pir* / pK18*mobsacB-Bd2052up-parS*$_{P1}$-*Bd2503down*	Kan	This study
GL669	TOP10 / pK18*mobsacB*	Kan	Lab collection
GL671	S17-1 λ*pir* / pK18*mobsacB-dnaNup-dnaN-msfgfp-dnaNdown*	Kan	This study
GL726	MG1655 / pBAD18-*msfgfp*	Amp	This study
GL727	MG1655 / pBAD18-*mcherry*	Amp	This study
GL728	DH5α / pBG18 (pSEVA251-*pBioFab-sfgfp*)	Kan	Kind gift from C. Lesterlin (U. Lyon)
GL743	S17-1 λ*pir* / pTNV215-*cfp-parB*$_{P1}$	Gm	This study
GL744	S17-1 λ*pir* / pTNV215-*yfp-parB*$_{PMT1}$	Gm	This study
GL745	S17-1 λ*pir* / pTNV215-*yfp-parB*$_{PMT1}$- *cfp-parB*$_{P1}$	Gm	This study
GL809	S17-1 λ*pir* / pTNV215-*cfp-parB*$_{P1}$-*romR-tdtomato*	Gm	This study
GL831	S17-1 λ*pir* / pK18*mobsacB-parB*$_{Bb}$*up-parB*$_{Bb}$*-msfgfp-parB*$_{Bb}$*down*	Kan	This study
GL832	S17-1 λ*pir* / pK18*mobsacB-parB*$_{Bb}$*up-parB*$_{Bb}$*-mcherry-parB*$_{Bb}$down	Kan	This study
GL917	S17-1 λ*pir* / pTNV215-*parB*$_{Bb}$*-mcherry*	Gm	This study
GL918	S17-1 λ*pir* / pTNV215-*parB*$_{Bb}$*-msfgfp*	Gm	This study
GL972	S17-1 λ*pir* / pK18*mobsacB-Bd0063-pBioFab-sfgfp-Bd0064*	Kan	This study
GL974	S17-1 λ*pir* / pK18*mobsacB-Bd0063-pBioFab-sfTq2ox-Bd0064*	Kan	This study
GL975	S17-1 λ*pir* / pK18*mobsacB-Bd0063-pBioFab-mcherry-Bd0064*	Kan	This study
GL985	S17-1 λ*pir* / pTNV215-*parB*$_{Bb}$	Gm	This study
GL1001	S17-1 λ*pir* / pTNV215-*mcherry-parB*$_{PMT1}$	Gm	This study
GL1223	TOP10 / pTNV215-*msfgfp*	Gm	This study
GL1263	S17-1 λ*pir* / pTNV215-*yfp-parB*$_{PMT1}$- *parB*$_{Bb}$*-mcherry*	Gm	This study
GL1314	S17-1 λ*pir* / pK18*mobsacB-dnaXup-dnaX-msfgfp-dnaXdown*	Kan	This study
GL1420	S17-1 λ*pir* / pTNV215-*PBd3471-cfp-parB*$_{P1}$	Gm	This study
GL1424	S17-1 λ*pir* / pTNV215-*PBd3471-yfp-parB*$_{PMT1}$	Gm	This study

CJW6321	MG1655 *seqA*::*seqA-mcherry,* constructed as CJW6324 in [S4], here without the *ftsZ-venus*^{SW} fusion	/	Kind gift from C. Jacobs-Wagner (Stanford U.)
MT4401	TOP10 / pMT679 (used to amplify *mcherry*)	Chlor	[S5]
/	DH5α / pNM077 (used to amplify *sftq2ox* encoding monomeric superfolder Turquoise2ox)	Amp	[S6]
/	TOP10 / pTNV162 (used to amplify *msfgfp* encoding monomeric superfolder GFP)	Amp	[S7]
/	TOP10 / pTNV167 (used to amplify *msfgfp* encoding monomeric superfolder GFP)	Amp	Kind gift from L. Hamoen (U. Amsterdam)
/	TOP10 / pTNV143 (used to amplify *msfgfp* encoding monomeric superfolder GFP)	Amp	Kind gift from L. Hamoen (U. Amsterdam)

Table S1. Strain information: *E. coli* and *Bdellovibrio bacteriovorus* strains used in this study. Related to STAR Methods. *pBioFab is a constitutively active synthetic promoter; **PBd3471 is a *B. bacteriovorus* promoter active in attack phase[S8].

Plasmid description	Method of construction
pMQ414-*romR*, gm^R	Assembly of *romR* (*Bd2761*) PCR-amplified from purified HD100 gDNA (oGL206/oGL207) with EcoRI-digested pMQ414 (GL495).
pTNV215-*tdtomato*, gm^R	Assembly of PCR fragments of pMQ414 amplified with primers oGL283/oGL296, oGL281/oGL284, oGL280/oGL282, resulting in the removal of yeast maintenance elements from pMQ414 (GL495).
pTNV215-*romR-tdtomato*, gm^R	Assembly of PCR fragments of pMQ414-*romR* amplified with primers oGL281/oGL283 and oGL280/oGL282, resulting in the removal of yeast maintenance elements from pMQ414-*romR* (GL511).
pK18*mobsacB-Bd3895up-parS$_{PMT1}$-Bd3896down*, kan^R	Assembly of the following DNA fragments: *Bd3895up* amplified from HD100 gDNA using primers oGL227/oGL228; *parS$_{PMT1}$* amplified from plasmid in GL506 using primers oGL229/oGL230; *Bd3895down* amplified from HD100 gDNA using primers oGL231/oGL232; XbaI-digested pK18*mobsacB* (GL669).
pK18*mobsacB-Bd2052up-parS$_{P1}$-Bd2053down*, kan^R	Assembly of the following DNA fragments: *Bd2052up* amplified from HD100 gDNA using primers oGL233/oGL234; *parS$_{P1}$* amplified from plasmid in GL507 using primers oGL235/oGL236; *Bd2053down* amplified from HD100 gDNA using primers oGL237/oGL238; XbaI-digested pK18*mobsacB* (GL669).
pK18*mobsacB-dnaNup-msfgfp-dnaNdown*, kan^R	Assembly of the following PCR-amplified fragments: *Bd0002* amplified from HD100 gDNA using primers oGL395/oGL396; *msfgfp* amplified with oGL299/oGL300 from pTNV167 (GL597); *dnaNdown* amplified from HD100 gDNA using primers oGL397/oGL398; vector pK18*mobsacB* (GL669) amplified with primers oGL331/oGL332.
pBAD18-*msfgfp*, amp^R	Assembly of PCR fragments amplified from pBAD18 with primers oGL321/oGL322, and from pTNV162 with primers oGL340/oGL326
pBAD18-*mcherry*, amp^R	Assembly of PCR fragments amplified from pBAD18 with primers oGL321/oGL322, and from pMT679 with primers oGL330/oGL509
pTNV215-*cfp-parB$_{P1}$*, gm^R	Assembly of the following PCR-amplified fragments: *PnptII* amplified from pPROBE-NT vector (strain GL573) using primers oGL287/oGL288; *cfp-parB$_{P1}$* amplified from plasmid in GL505 using primers oGL289/oGL559; pTNV215 vector amplified from pTNV215-*tdtomato* (GL606) using primers oGL451/oGL452.
pTNV215-*yfp-parB$_{PMT1}$*, gm^R	Assembly of the following PCR-amplified fragments: *PnptII* amplified from pPROBE-NT vector (strain GL573) using primers oGL287/oGL288; *yfp-parB$_{PMT1}$* amplified from plasmid in GL504 using primers oGL291/oGL560; pTNV215 vector amplified from pTNV215-*tdtomato* (GL606) using primers oGL451/oGL452.
pTNV215-*yfp-parB$_{PMT1}$-cfp-parB$_{P1}$*, gm^R	Assembly of the following PCR-amplified fragments: *PnptII* amplified from pPROBE-NT vector (strain GL573) using primers oGL287/oGL288; *yfp-parB$_{PMT1}$* amplified from plasmid in GL504 using primers oGL291/oGL295; *cfp-parB$_{P1}$* amplified from plasmid in GL505 using primers oGL293/oGL559; pTNV215 vector amplified from pTNV215-*tdtomato* (GL606) using primers oGL451/oGL452.
pTNV215-*cfp-parB$_{P1}$-romR-tdtomato*, gm^R	Assembly of the following PCR-amplified fragments: *romR-tdtomato* amplified from pTNV215-*romR-tdtomato* (GL611) using primers oGL702/oGL703; *cfp-parB$_{P1}$* amplified from plasmid in GL743 using primers oGL700/oGL701; pTNV215 vector amplified from pTNV215-tdtomato (GL606) using primers oGL451/oGL452.
pK18*mobsacB-parB$_{Bb}$up-parB$_{Bb}$-mcherry-parB$_{Bb}$down*, kan^R	Assembly of the following PCR-amplified fragments: *Bd3905up* amplified from HD100 gDNA of HD100 using primers oGL751/oGL752; *mcherry* amplified from plasmid in GL701 using primers oGL489/oGL209; *Bd3905down* amplified from HD100 gDNA using primers oGL755/oGL754; pK18*mobsacB* (GL669) amplified using primers oGL331/oGL332.

pK18*mobsacB-parB$_{Bb}$up-parB$_{Bb}$-msfgfp-parB$_{Bb}$down,* kan^R	Assembly of the following PCR-amplified fragments: *Bd3905up* amplified from HD100 gDNA using primers oGL751/oGL752; *msfgfp* amplified using primers oGL299/oGL337 from pTNV167 (GL597); *Bd3905down* amplified from HD100 gDNA using primers oGL753/oGL754; pK18*mobsacB* (GL669) amplified using primers oGL331/oGL332.
pTNV215-*parB$_{Bb}$-mcherry*, gm^R	Assembly of *parB$_{Bb}$-mcherry* amplified from plasmid in GL831 using primers oGL890/oGL891, and pTNV215 vector amplified from pTNV215-*tdtomato* (GL606) using primers oGL451/oGL452.
pTNV215-*parB$_{Bb}$-msfgfp*, gm^R	Assembly of *parB$_{Bb}$-msfgfp* amplified from plasmid in GL832 using primers oGL890/oGL892, and pTNV215 vector amplified from pTNV215-*tdtomato* (GL606) using primers oGL451/oGL452.
pK18*mobsacB-Bd0063-pBioFab-sfgfp-Bd0064*, kan^R	Assembly of the following PCR fragments: *Bd0063* amplified from HD100 gDNA using primers oGL961/oGL962; *pBioFab-sfgfp* amplified with oGL963/oGL964 from pBG18 (GL728); *Bd0064* amplified from HD100 gDNA using primers oGL965/oGL966; vector pK18*mobsacB* (GL669) amplified with primers oGL264/oGL265.
pK18*mobsacB-Bd0063-pBioFab-sftq2ox-Bd0064*, kan^R	Assembly of sft*q2ox* amplified from plasmid pNM077 (GL601) using primers oGL887/oGL968, and a vector fragment amplified from pK18*mobsacB-Bd0063-pBioFab-sfgfp-Bd0064* (GL976) with primers oGL783/oGL967.
pK18*mobsacB-Bd0063-pBioFab-mcherry-Bd0064*, kan^R	Assembly of *mcherry* amplified from plasmid in GL832 using primers oGL887/oGL968, and a vector fragment amplified from pK18*mobsacB-Bd0063-pBioFab-sfgfp-Bd0064* (GL976) with primers oGL783/oGL967.
pTNV215-*parB$_{Bb}$,* gm^R	Assembly of *parB$_{Bb}$* amplified from HD100 gDNA using primers oGL890/oGL952, and. pTNV215 vector amplified from pTNV215-*tdtomato* (GL606) using primers oGL451/oGL452.
pTNV215-*mcherry-parB$_{PMT1}$,* gm^R	Assembly of *mcherry* amplified from plasmid in GL832 using primers oGL491/oGL338, and a fragment from plasmid in GL744 amplified using primers oGL452/oGL973.
pTNV215-*msfgfp,* gm^R	Assembly of PCR fragments amplified from pTNV215-*tdtomato* (GL606) with primers oGL282/oGL362, and from pTNV143 (GL598) amplified with primers oGL363/oGL364
pTNV215-*yfp-parB$_{PMT1}$-parB$_{Bb}$-mcherry*, gm^R	Assembly of *parB$_{Bb}$-mcherry* amplified from plasmid in GL917 using primers oGL1117/oGL1118, and plasmid in GL744 amplified using primers oGL1116/oGL451.
pK18*mobsacB-dnaXup-dnaX-msfgfp-dnaXdown*, kan^R	Assembly of the following PCR-amplified fragments: *Bd3731* amplified from HD100 gDNA using primers oGL520/oGL521; *msfgfp* amplified with oGL299/oGL300 from pTNV167 (GL597); *dnaXdown* amplified from HD100 gDNA using primers oGL522/oGL523; vector pK18*mobsacB* (GL669) amplified with primers oGL331/oGL332.
pTNV215-*PBd3417-cfp-parB$_{P1}$,* gm^R	Assembly of the following PCR-amplified fragments: *PBd3471* amplified from HD100 gDNA using primers oGL1302/oGL1303; pTNV215-c*fp-ParB$_{P1}$* amplified with oGL1298/oGL1299, resulting in the replacement of the constitutively active PnptII promoter by the PBd3471 promoter.
pTNV215-*PBd3417-yfp-parB$_{PMT1}$,* gm^R	Assembly of the following PCR-amplified fragments: *PBd3471* amplified from HD100 gDNA using primers oGL1302/oGL1303; pTNV215-y*fp-ParB$_{PMT1}$* amplified with oGL1298/oGL1299, resulting in the replacement of the constitutively active PnptII promoter by the PBd3471 promoter.

Table S2. Construction of plasmids used in this study. Related to STAR Methods.

Bdellovibrio bacteriovorus	
Strains	**Construction method**
GL512	Mating GL499 x GL511
GL673	Mating GL499 x GL671, allelic replacement
GL676	Mating GL734 x GL631, allelic replacement
GL771	Mating GL676 x GL743
GL772	Mating GL676 x GL744
GL773	Mating GL676 x GL745
GL784	Mating GL734 x GL743
GL785	Mating GL734 x GL744
GL806	Mating GL734 x GL630, allelic replacement
GL816	Mating GL676 x GL809
GL867	Mating GL806 x GL743
GL868	Mating GL806 x GL744
GL869	Mating GL806 x GL745
GL870	Mating GL806 x GL809
GL906	Mating GL734 x GL832, allelic replacement
GL909	Mating GL806 x GL631, allelic replacement
GL995	Mating GL909 x GL745
GL1002	Mating GL734 x GL917
GL1003	Mating GL734 x GL918
GL1004	Mating GL734 x GL919
GL1023	Mating GL734 x GL977, allelic replacement
GL1024	Mating GL734 x GL978, allelic replacement
GL1025	Mating GL734 x GL979, allelic replacement
GL1055	Mating GL906 x GL671, allelic replacement
GL1102	Mating GL806 x GL671, allelic replacement
GL1103	Mating GL1102 x GL1001
GL1121	Mating GL906 x GL630, allelic replacement
GL1211	Mating GL673 x GL612
GL1212	Mating GL734 x GL976, allelic replacement
GL1122	Mating GL906 x GL631, allelic replacement
GL1261	Mating GL734 x GL985
GL1364	Mating GL499 x GL1314, allelic replacement
GL1367	Mating GL1121 x GL744
GL1368	Mating GL1122 x GL743
GL1372	Mating GL806 x GL1263
GL1388	Mating GL1025 x GL918
GL1475	Mating GL1420 x GL771
GL1476	Mating GL1424 x GL868

Table S3. Construction of *Bdellovibrio bacteriovorus* strains used in this study. Related to STAR Methods.

Primer name	Primer sequence (5'>3')
oGL060	cattcgccattcaggctgc
oGL206	**tcaagagacaggatgaggag**AATTCCATATGGCTTTACGCGTCTTGC
oGL207	**ctcgcccttgctcaccatg**AGCTCAAGCTTGGTACCAATGGACTTTTCAGTTTCGCG
oGL209	TTACTTGTACAGCTCGTCCAT
oGL229	**gatattctgaaaa**TGTTTTTCACCACGCCAATTTC
oGL230	**gcctccgtttctt**GAGGTTGAAAAGCGTGGTG
oGL231	**gcttttcaacctc**AAGAAACGGAGGCTTGTG
oGL232	**aagcttgcatgcctgcaggtcgact**AGCTAAGAAGCTGCAGGC
oGL233	**ttcgagctcggtacccggggatcct**TCAACTCTTTGGGATATGG
oGL234	**atggcgaaagttt**ACTGGCTTTTTTGTTTTATC
oGL235	**caaaaaagccagt**AAACTTTCGCCATTCAAATTTC
oGL236	**tcaggatccccgg**CCAAGGTGAAATCGTGGC
oGL237	**gatttcaccttgg**CCGGGGATCCTGACTGGC
oGL238	**aagcttgcatgcctgcaggtcgact**AGTTCCGACGGCGAACTTC
oGL244	attgtgagcggataaca
oGL257	cagtaccgggatgagatctt
oGL258	cttgccaatatcgctgacct
oGL264	TCTAGAGTCGACCTGCAG
oGL265	GGATCCCCGGGTACCGAG
oGL280	**ctggccgataagctccacgtg**GTGATGAAAAGGACCCAGGTGGCA
oGL281	cctctccccgcgcgttggccgattca
oGL282	gaattctcctcatcctgtctcttgatca
oGL283	gtggagcttatcggccagcctcgca
oGL284	ggaccaccgcgctactgccgccaggca
oGL287	**cgactctagaggatccccgggtacc**CCCGGGACGCTGCCGCAA
oGL288	gaattctcctcatcctgtctct
oGL289	**tcaagagacaggatgaggagaattc**ATGAGTAAAGGAGAAGAACTTTT
oGL291	**tcaagagacaggatgaggagaattc**ATGTCTAAAGGTGAAGAACTGTT
oGL293	ggaaagacttccagaatcaggtgagt
oGL295	cctgattctggaagtctttccagaa
oGL296	gcctggcggcagtagcgcggtggt
oGL299	**ggctcaggaagcggctcagg**ATCCAAAGGA
oGL300	**ccgcgctactgccgccaggc**GGTAGCGACCGGCGCTCAGAGCTTGA
oGL304	ggtgataccctggtgaaccgtat
oGL305	ggtctgcgtttgatgcgaatgaa
oGL306	gcgagctggggaagcgactcgaa
oGL316	cagagtcccgctcagaagaactcgt
oGL331	ggcactggccgtcgttttacaa
oGL332	gtaatcatgtcatagctgtttcctgtgtgaaa
oGL338	**ggatcctgagccgcttcctgagcc**CTTGTACAGCTCGTCCATGCC

oGL343	gccttctatcgccttcttgacga
oGL344	gcaaaaggcctggacgtttggga
oGL345	ggcccatacaagccgctgaacaaaa
oGL346	gccaaagggttcgtgtagact
oGL354	gcaaccatttcgtctggcactgct
oGL355	gcagacctatttctcgaatgct
oGL371	**agacaggatgaggagaattcatg**GCATTATTACTGGTCAGCGCCT
oGL381	ccgaccaagcgacgcccaacctgcca
oGL382	ttcttctgagcgggactctgcacatatacctgccgttcactattat
oGL383	gttgggcgtcgcttggtcggttatttgttaactgttaattgtccttgt
oGL387	cgggtaccgagctcgaattcgt
oGL388	ttcgagctcggtacccggggatcct
oGL389	ttcgagctcggtacccggggatcctggaagatgaagtcctgtcccagaatttaaa
oGL390	**cgggtaccgagctcgaattc**GTGCCAAGCTTGCATGCCTGCAGGTCGA
oGL391	**ttcgagctcggtacccggggatc**CTTCAACTCTTTGGGATAT
oGL392	**cgggtaccgagctcgaattcgt**CCAAGCTTGCATGCCTGCAGGTCGACTAGTT
oGL395	**acagctatgacatgattacg**GGTGTGATCATTCCaCGCAAAGGT
oGL396	**ggatcctgagccgcttcctgagcc**GATTCTCATTGGCATCACAACGCA
oGL397	**gcctggcggcagtagcgcgg**CCTCACAACGACCAGACTTACA
oGL398	**gtaaaacgacggccagtgcc**TTCAGCGCTTTTCGGTAATC
oGL447	atgtctgatattgctgt
oGL448	ttactgccatccttctttaa
oGL451	ggatcctgatacagattaaatcagaacgcag
oGL452	gaattctcctcatcctgtctcttgatcag
oGL489	**ggaagcggctcaggatcc**GTGAGCAAGGGCGAGGAG
oGL491	**agacaggatgaggagaattc**ATGGTGAGCAAGGGCGAG
oGL498	gaagagcgcccaatacgca
oGL520	**cctgagccgcttcctgagcc**GTGGCCGCGCTTGTTCAGTTCAACGA
oGL521	**acagctatgacatgattac**CCCTCTCACAGCGCAGGTGGGGCCA
oGL522	**gtaaaacgacggccagtgcc**GCGGCAGATATCCGTGTCGGTGTAGT
oGL523	**gcctggcggcagtagcgcgg**GCCGCTCAAACCGTGTTCAAGGGACA
oGL559	**ctgcgttctgatttaatctgtatcaggatcc**TTAAGGCTTCGGCTTTTTATCGA
oGL560	**ctgcgttctgatttaatctgtatcaggatcc**TTACTCACCTGATTCTGGAAGTC
oGL638	gagtacgacagcaaatccat
oGL639	catctctttcacagagtcagg
oGL681	**tcaagagacaggatgaggagaattc**ATGAGTAAAGGAGAAGAACT
oGL682	**tctgatttaatctgtatcaggatcccta**TTTATACAGCTCATGCA
oGL699	gtaaccgagttcgcggcgggcaa
oGL700	ctgtacaagtaaaagcggtctgataaaacagaatttgc
oGL701	tggaattctcctcttaaggcttcggctttttatcgagg
oGL702	**ccgaagccttaagagga**GAATTCCATATGGCTTTACGC
oGL703	tatcagaccgcttttacttgtacagctcgtccatgcc

oGL704	ctgtacaagtaactggcggcagtagcgcg
oGL705	**tggaattctcct**CTTACTCACCTGATTCTGGAAGTCTTTCC
oGL706	**tcaggtgagtaagaggag**AATTCCATATGGCTTTACGC
oGL707	**ctactgccgccag**TTACTTGTACAGCTCGTCCATGCC
oGL708	gttgtcctcggaggaggc
oGL709	tgaactctttgatgacctcctc
oGL751	**cacacaggaaacagctatgacatgatta**CGAGTACGACAGCAAATCCAT
oGL752	**atcctgagccgcttcctgagc**CCTGCCATCCTTCTTTAAGCCT
oGL753	**acatggcatggatgagctctacaaa**TAGGGTTTGAGCGATGAGCTTCAGAAAA
oGL754	**gtaaaacgacggccagtgcc**GCATTGGCGGCCTGAACAG
oGL755	**ggcatggacgagctgtacaagtaa**GGTTTGAGCGATGAGCTTCAGAAAA
oGL783	CATATTCACCACCCTGAATTGACTCTCTT
oGL809	gatacctagttgtgcaaaaatgt
oGL810	gtggtcttgacctcagcgtc
oGL811	gacatcacctcccacaacg
oGL887	**aattcagggtggtgaatatg**GTGAGCAAGGGCGAG
oGL890	**tcaagagacaggatgaggagaattc**ATGTCTGATATTGCTGTAGAAT
oGL891	**tctgatttaatctgtatcaggatcc**TTACTTGTACAGCTCGTCCAT
oGL892	**tctgatttaatctgtatcaggatcta**TTTGTAGAGCTCATCCATGC
oGL893	**tggaatt**CTCCTCTTACTTGTACAGCTCGTCCAT
oGL894	**agctgtacaagtaagaggag**AATTCCATATGGCAAAAACAATCTGCAT
oGL952	**ctgatttaatctgtatcaggatcctta**TTACTGCCATCCTTCTTTA
oGL961	**tacgaattcgagctcggtacccggggatcc**ATCAGAACTGTTTCCAAAAACCTTCTGG
oGL962	**atactctatcgatgcctcgctcttttctttt**TTTGGAGAACCC
oGL963	**aaagaaaagagcgaggcatcgatagagtat**TGACTTCGC
oGL964	**aagagcgagtgaaaattatttgtagagctc**ATCCATGCCG
oGL965	**gagctctacaaataa**TTTTCACTCGCTCTTTTTGTTTTTGCG
oGL966	**aagcttgcatgcctgcaggtcgactctaga**AGATTGTTCATAATGTTCGAGGGTTTAACAC
oGL967	ttttcactcgctcttttgtttttgcg
oGL968	**acaaaaagagcgagtgaaaa**TTACTTGTACAGCTCGTCCATGC
oGL973	**ggctcaggaagcggctcaggatc**CGGCGACGGTGATGTTAAAA
oGL1116	ttactcacctgattctggaagtctttcc
oGL1117	**aagacttccagaatcaggtgagtaa**GATCAAGAGACAGGATGAGGAGAATTCATGTCTGATAT
oGL1118	**tctgatttaatctgtatcaggatcc**TTACTTGTACAGCTCGTCCATGCCG
oGL1298	tcaagagacaggatgaggagaat
oGL1299	cccgggccagctgcattaat
oGL1302	**gattcattaatgcagctggcccgg**GTATTTTTTCATGCCAGCGA
oGL1303	**gaattctcctcatcctgtctcttga**TGTATACGCCTTTCAAAG

Table S4. Oligos used in this study. Related to STAR Methods. Overlapping sequences used for cloning by DNA assembly are highlighted in black.

Supplemental References

S1. Rendulic, S., Jagtap, P., Rosinus, A., Eppinger, M., Baar, C., Lanz, C., Keller, H., Lambert, C., Evans, K.J., Goesmann, A., et al. (2004). A predator unmasked: life cycle of Bdellovibrio bacteriovorus from a genomic perspective. Science *303*, 689–692. 10.1126/science.1093027.

S2. Deghelt, M., Mullier, C., Sternon, J.-F., Francis, N., Laloux, G., Dotreppe, D., Van der Henst, C., Jacobs-Wagner, C., Letesson, J.-J., and De Bolle, X. (2014). G1-arrested newborn cells are the predominant infectious form of the pathogen Brucella abortus. Nat Comms *5*, 4366. 10.1038/ncomms5366.

S3. Miller, W.G., Leveau, J.H., and Lindow, S.E. (2000). Improved gfp and inaZ broad-host-range promoter-probe vectors. Mol. Plant Microbe Interact. *13*, 1243–1250. 10.1094/MPMI.2000.13.11.1243.

S4. Gray, W.T., Govers, S.K., Xiang, Y., Parry, B.R., Campos, M., Kim, S., and Jacobs-Wagner, C. (2019). Nucleoid size scaling and intracellular organization of translation across bacteria. Cell *177*, 1632–1648.e20.

S5. Thanbichler, M., Iniesta, A.A., and Shapiro, L. (2007). A comprehensive set of plasmids for vanillate- and xylose-inducible gene expression in Caulobacter crescentus. Nucleic Acids Res. *35*, e137. 10.1093/nar/gkm818.

S6. Meiresonne, N.Y., Consoli, E., Mertens, L.M.Y., Chertkova, A.O., Goedhart, J., and Blaauwen, Den, T. (2019). Superfolder mTurquoise2ox optimized for the bacterial periplasm allows high efficiency in vivo FRET of cell division antibiotic targets. Mol. Microbiol. *111*, 1025–1038. 10.1111/mmi.14206.

S7. Saaki, T.N.V., Strahl, H., and Hamoen, L.W. (2018). Membrane curvature and the Tol-Pal complex determine polar localization of the chemoreceptor Tar in Escherichia coli. J. Bacteriol. *200*. 10.1128/JB.00658-17.

S8. Karunker, I., Rotem, O., Dori-Bachash, M., Jurkevitch, E., and Sorek, R. (2013). A global transcriptional switch between the attack and growth forms of Bdellovibrio bacteriovorus. PLoS ONE *8*, e61850. 10.1371/journal.pone.0061850.